

The magnetic structure of $\text{Er}_2\text{Ti}_2\text{O}_7$

A.K.R. Briffa, R.J. Mason, and M.W. Long

School of Physics, Birmingham University, Edgbaston, Birmingham, B15 2TT, United Kingdom.

(Dated: November 21, 2018)

We employ the previously published neutron scattering experiments[1–3] to suggest that $\text{Er}_2\text{Ti}_2\text{O}_7$ has a broken-symmetry multiple- \mathbf{q} state with tetragonal magnetic symmetry[4]. The ordered moments do not appear to lie close to the crystal-field anticipated directions[5] and we suggest that the low energy gapless mode, visible in specific-heat measurements[6], is not of the usual transverse isotropic Goldstone-mode type, but is longitudinal and is associated with the internal transfer of magnetism between distinct magnetic Bragg spots.

PACS numbers: 03.75.Lm, D75.25.+z, 75.30.Ds

I. INTRODUCTION

There is currently a lot of experimental and theoretical interest in rare-earth pyrochlore magnets of stoichiometry, $\text{R}_2\text{M}_2\text{O}_7$, where R is a rare-earth atom and M is an atom that has an available M^{4+} state, such as tin or titanium. Much of the interest has focused on ‘spin-ice’[7], the $\text{Ho}_2\text{Ti}_2\text{O}_7$ and $\text{Dy}_2\text{Ti}_2\text{O}_7$ compounds, due to the proposal that they can be considered to be analogue ‘monopole’ systems[8]. The original motivation for studying these systems was the macroscopic degeneracy expected for the isotropic Heisenberg model[9]. The compounds $\text{Gd}_2\text{Ti}_2\text{O}_7$ [10] and $\text{Gd}_2\text{Sn}_2\text{O}_7$ [11] are systems that are expected to conform to this model at intermediate temperature. The issue of how this residual degeneracy is lifted at very low temperature then surfaced and further work understanding the dipolar interaction was then relevant[12]. Spin-ice is a system with a strong crystal-field interaction forcing the spins to point along the natural crystallographic directions whereas the gadolinium compounds have essentially no anticipated crystal field (subject to some unexpected ESR issues[13]). To complete the set it would be nice to have a material where the local crystal-field promoted spins perpendicular to the natural crystallographic directions, and the compound $\text{Er}_2\text{Ti}_2\text{O}_7$ was thought to play this role[14]. Theoretical crystal-field calculations[5], neutron scattering experiments[1–3] and specific heat measurements[6] were all brought forward to promote this picture. Indeed, a subtle ‘order from disorder’ calculation[15] appeared to predict the observed experiments. In this article we offer an alternative view that the spins are oriented quite close to the natural crystallographic axes, but are actually slightly distorted away into a point-symmetry broken orientation. This loss of point-symmetry then leads to a continuous degeneracy which explains the anomalous entropy still present at low temperatures.

Our proposal for the physics of $\text{Er}_2\text{Ti}_2\text{O}_7$ is essentially equivalent to previous studies of multiple- \mathbf{q} magnetism in face-centre-cubic magnets[4], which contain most of the fundamental ideas and concepts. We organise the paper into three main sections; firstly a discussion of the main experiments and how they lead us to our proposed ground-state, secondly a theoretical model that can be

used to understand the majority of the experiments and thirdly a semi-classical spinwave analysis of our model. Our model is clearly only approximately solved which causes clear ‘gaps’ in our reasoning. Finally we conclude.

II. EXPERIMENTS AND INTERPRETATION

We commence with the specific heat measurements[6], which have been repeated as a function of field[2, 3, 16], although the original measurements are all that we require. These specific heat measurements lead directly to three crucial physical facts. Firstly there is a clear phase transition near in energy to the natural dipolar energy-scale[14]. Secondly there are only two states per atom involved in this low temperature phase transition, a Kramer’s doublet, and so we need only deal with a pseudo-spin half. Thirdly the relevant low temperature magnetic contribution is gapless and the observed power-law is consistent with a magnon dispersion that goes linearly to zero at isolated points in reciprocal-space. It is this third point which is totally unexpected: spin-orbit interactions provide a coupling between the spin direction and the lattice which almost invariably lead to a spinwave gap. In transition metals the spin-orbit interaction is weak in comparison to the exchange[17] and so the gap is small, but in rare-earth magnets this interaction is usually huge and any associated low energy mode is absent. The only likely failure for this argument is when the atom has a pure isotropic spin, gadolinium for example, where this anisotropy might be expected to be absent. Erbium would be expected to have a huge anisotropy gap. Sometimes low energy modes are seen (although not vanishing), in CeAs for example[18], however the interpretation for these modes is different[4]. These special modes occur in multiple- \mathbf{q} magnetism, only found in frustrated systems whose magnetism breaks the point-group symmetry of the underlying crystal. The modes are associated with transferal of spin-density between distinct Bragg spots and correspond to local spin rotations which are longitudinal antiferromagnetic in character. We are proposing that it is one of these special modes that has gone soft in $\text{Er}_2\text{Ti}_2\text{O}_7$.

The most important experiments for our development

are those involving neutrons. There is a powder diffraction experiment[1], a single-crystal diffraction experiment in a restricted plane but with critical inelastic measurements[2], a fairly complete single-crystal diffraction experiment[3] and a polarised neutron study[19]. We will deal with the elastic scattering first and then consider the inelastic separately. Elementary investigation of neutron scattering data involves three critical elements: the structure-factor, the form-factor and the orientational-factor. The structure-factor variation stems from the different moment directions occurring on distinct atoms in the magnetic unit cell, and for us is fairly definitive. The form-factor arises from the orbital spread of the magnetic moment about the site of the nucleus, and is both a complication and a concern. The magnetic erbium core is in a very complicated state, dominated by Hund's rules, it has a maximal total angular momentum which is parallel to its maximal spin to provide $J = 15/2$. The sixteen states are crystal field split to a relevant pseudo-spin doublet. The additional crystal-field doublets are visible using inelastic neutron scattering[1], but are at high energies in comparison to the inate energy of the phase transition. Indeed, the specific-heat measurements yield almost precisely this pseudo-spin degeneracy before the higher energy states impinge[6]. These complex low energy states have a shape that will distort the form-factor[20]. We will ignore this distortion and presume that the form-factor is spherically symmetric. This issue is usually not a worry, because domain averaging reinstates the point-symmetry, however our proposed magnetism breaks that point-symmetry and would highlight these effects. The orientational-factor (that stems from the fact that neutrons can only scatter from moments perpendicular to the direction of momentum transfer) is very physically informative and marks the start of our analysis.

In simple terms, for any set of spots with the same structure-factor, one looks for the smallest (form-factor compensated) spot. The magnetic moment associated with that structure-factor is then essentially parallel to the reciprocal-lattice-vector, \mathbf{G} , of that spot. The neutron-scattering data then provides the following information. The closest spots to the origin, (111) , $(1\bar{1}\bar{1})$, $(\bar{1}\bar{1}1)$ $(\bar{1}\bar{1}1)$, are all quite small. The second-closest spots to the origin, (200) , (020) and (002) are all very small, while the third-closest spots, (022) , (202) and (220) , are dominant. The second observation is crucial, since it tells us that the three independent components of spin-density that characterise the magnetism are parallel to the Cartesian directions. The states are described mathematically by

$$\mathbf{m}(\mathbf{R}) = |\mathbf{m}| \left[e^{\hat{\mathbf{x}} \cdot \mathbf{R} 2\pi i} \sin \theta \cos \phi \hat{\mathbf{x}} + e^{\hat{\mathbf{y}} \cdot \mathbf{R} 2\pi i} \sin \theta \sin \phi \hat{\mathbf{y}} + e^{\hat{\mathbf{z}} \cdot \mathbf{R} 2\pi i} \cos \theta \hat{\mathbf{z}} \right] \quad (1)$$

where \mathbf{R} is the position of the atom in natural units (corresponding to the underlying face-centre-cubic Bravais lattice) and pictorially by Fig.1. To limit to the depicted magnetism, we also require that there is no ferromagnetism in the system, which is controlled by

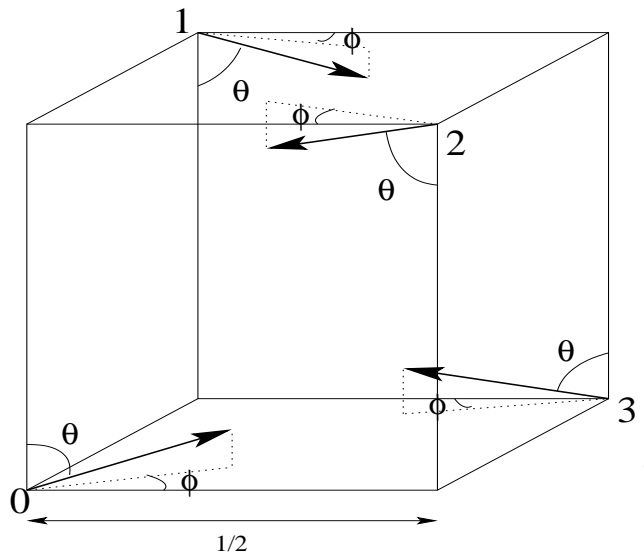


FIG. 1: The spin-states consistent with vanishing Bragg spots (200) , (020) and (002) .

the almost vanishing (222) Bragg spot. Technically, these states are equivalent to Type I face-centre-cubic antiferromagnetism[4], but interestingly, the pyrochlore magnetism is easier to deduce than that of face-centre-cubic. The key observation is that the (111) spots provide complementary information: this particular spot provides a phase which splits the lattice up into planes perpendicular to the (111) direction, each of which has uniform phase. These planes happen to be alternating Kagomé and sparse triangular planes with alternating signs. The key observation is that these triangular planes make up one of the four sublattices, while the Kagomé planes make up the other three. If the system is an antiferromagnet, then the structure factor for this Bragg spot should be proportional to the spin direction on the triangular sublattice. The experimental observation that the (111) Bragg spot is quite small then provides the information that the spin on site zero of Fig.1 is almost parallel to the (111) direction. This clearly contradicts the endemic idea that the spins are perpendicular to the natural crystallographic directions[1–3, 5, 14–16, 19].

The neutron experiments also clearly exhibit distinct magnetic domains[1–3]. This is clearly inconsistent with the idea that the state is a pure triple- \mathbf{q} state (spins pointing towards the natural crystallographic directions, defined by $\cos \Theta = \frac{1}{\sqrt{3}}$), because this state preserves the cubic symmetry. The magnetic field experiments provide us with an essentially unique state. The experimental evidence was initially conflicting; the first measurement[1] tried to imply domains from a jump in intensity for a single Bragg spot when a field was applied. Domains correspond to *redistribution* of Bragg intensity, and so if one peak grows then another should reduce, whereas a change in a single Bragg spot should signal a fundamental change in magnetism and *not* a change in domain struc-

ture. This experimental result was therefore anomalous until the single-crystal measurement[2] indicated an unexpected and unexplained diffuse peak that enlarged the Bragg spot with the inclusion of the field. This single-crystal work[2] does show clear indications of domains, but because not all of the magnetic Bragg scattering was observed it is not unambiguous. The final fairly complete measurement[3] measures all three crucial peaks independently and they are seen to separate in an intensity preserving way once the field is applied. We can fit the three intensities to our Eq.(1) and we find that

$$\tan \phi = 1 \quad \tan \theta \sim \frac{4}{3\sqrt{3}} \quad (2)$$

although no crystallographic significance should be attributed to our approximation. This direction is quite close to $\frac{1}{\sqrt{6}}(1, 1, 2)$, which also holds no special significance, unlike the previously proposed, $\frac{1}{\sqrt{6}}(1, 1, \bar{2})$, which is perpendicular to the natural crystallographic directions. We have also analysed the (111) spot[2] which appears consistent with this choice, subject to our crude choice of form-factor, a pure hydrogenic f -state. The state we propose has tetragonal magnetic symmetry and lies on the path that smoothly connects the pure triple- \mathbf{q} state to the single- \mathbf{q} state[4].

Finally, we consider the inelastic neutron scattering[2] together with an ESR experiment[16]. The low-energy gapless mode is clearly visible close to the magnetic Bragg spots, and a second almost flat mode is also visible. Perhaps the most intriguing observation is that when the field is applied these magnons disappear, but reappear close to other point-group related Bragg spots[2], a subtle domain issue that we do not currently try to explain. Note that the position of this Goldstone mode is exactly equivalent to that in single- \mathbf{q} CeAs[18] or indeed in USb[21] or UO₂[22], both of which are thought to be pure triple- \mathbf{q} states. In parallel to this, the ESR experiments[16] see analogous modes but chase them as a function of field. The physical surprise here is that it is the flat mode that softens and controls the loss of antiferromagnetism and not the low-energy Goldstone-mode as might naïvely be presumed. This is further evidence that the low energy mode is not of the usual type.

III. MODELLING

Modelling rare-earth magnetism properly is complicated. The dominance of Hund's rules makes the orbital nature of the states complex and the local crystal-field interactions destroy a simple isotropic-spin picture. In previous work the case of Gd₂Ti₂O₇[12] was considered, here we anticipate a pure spin with no orbital complications and natural models. In this section we develop a phenomenological model to try to describe the observed behaviour of the erbium compound, and the natural models are severely renormalised.

One major theoretical complication is the crystal-field interaction, which projects the original large- J states onto a pseudo-spin half representation that controls the low temperature phase transition. This projection strongly renormalises the interactions and hence corrupts intuition. One can provide some understanding using an elementary model for this projection. For a half-integer J we can easily show that the projection onto the states $|J, \pm J\rangle$ along the natural crystallographic directions, defined by,

$$\begin{aligned} \hat{\mathbf{z}}_0 &\equiv \frac{\hat{\mathbf{x}} + \hat{\mathbf{y}} + \hat{\mathbf{z}}}{\sqrt{3}} & \hat{\mathbf{z}}_1 &\equiv \frac{\hat{\mathbf{x}} - \hat{\mathbf{y}} - \hat{\mathbf{z}}}{\sqrt{3}} \\ \hat{\mathbf{z}}_2 &\equiv \frac{-\hat{\mathbf{x}} + \hat{\mathbf{y}} - \hat{\mathbf{z}}}{\sqrt{3}} & \hat{\mathbf{z}}_3 &\equiv \frac{-\hat{\mathbf{x}} - \hat{\mathbf{y}} + \hat{\mathbf{z}}}{\sqrt{3}} \end{aligned} \quad (3)$$

yields the mapping

$$\hat{\mathbf{J}}_\alpha \mapsto 2J\hat{\mathbf{z}}_\alpha \left(\hat{\mathbf{z}}_\alpha \cdot \hat{\mathbf{S}}_\alpha \right) \quad (4)$$

where $\hat{\mathbf{J}}_\alpha$ are the original angular-momentum operators and $\hat{\mathbf{S}}_\alpha$ are the pseudo-spin half operators. We can then project any bilinear Hamiltonian onto an effective spin-half model. For the case of Er₂Ti₂O₇ the moment along the crystallographic axes is thought to be small[5] and in addition the ordered moment is indeed observed to be small[1]. To analyse this system it therefore seems more natural to project onto the states $|J, \pm \frac{1}{2}\rangle$ using the following mapping:

$$\hat{\mathbf{J}}_\alpha \mapsto \left(J + \frac{1}{2} \right) \hat{\mathbf{S}}_\alpha - \left(J - \frac{1}{2} \right) \hat{\mathbf{z}}_\alpha \left(\hat{\mathbf{z}}_\alpha \cdot \hat{\mathbf{S}}_\alpha \right) \quad (5)$$

The role of the crystallographic axes is dominant in the first case, Eq.(4), and weakened in the second, Eq.(5). At bilinear order, our projection onto pseudo-spin is quite general, if the two coefficients in Eq.(5) are made parameters, depending only on the idea that the crystal-field is dominated by a single natural direction.

We develop five natural interactions in our modelling. Four stem solely from the crystallographic directions and bilinear coupling. The first, H_0 , has no pseudo-spin analogue, and the others, H_1 , H_2 and H_3 , provide the dominant spin interactions. The fifth interaction, H_4 , couples the spin to the lattice and is crucial to our modelling. We elect to derive these interactions by looking at the natural energies in our system.

The first energy we consider is the dipolar energy, this is not the strongest interaction as both exchange and residual crystal-field are expected to dominate, but it is very instructive. Working on a single tetrahedron, in the presence of dominant antiferromagnetic Heisenberg interactions, the local dipolar interaction can be shown to take the form of a linear combination of two contributions

$$\begin{aligned} H_4 = \frac{1}{2} &\left[\left(\hat{S}_0^x + \hat{S}_1^x - \hat{S}_2^x - \hat{S}_3^x \right)^2 \right. \\ &+ \left(\hat{S}_0^y - \hat{S}_1^y + \hat{S}_2^y - \hat{S}_3^y \right)^2 \\ &\left. + \left(\hat{S}_0^z - \hat{S}_1^z - \hat{S}_2^z + \hat{S}_3^z \right)^2 \right] \end{aligned} \quad (6)$$

and

$$H_0 = \frac{1}{6} \left[\left(\hat{S}_0^x + \hat{S}_0^y + \hat{S}_0^z \right)^2 + \left(\hat{S}_1^x - \hat{S}_1^y - \hat{S}_1^z \right)^2 \right. \\ \left. + \left(-\hat{S}_2^x + \hat{S}_2^y - \hat{S}_2^z \right)^2 + \left(-\hat{S}_3^x - \hat{S}_3^y + \hat{S}_3^z \right)^2 \right] \\ \equiv \frac{1}{2} \sum_{\alpha} \left(\hat{\mathbf{z}}_{\alpha} \cdot \hat{\mathbf{S}}_{\alpha} \right)^2 \quad (7)$$

where the coefficient of H_0 is six times that of H_4 for the local interaction. Using Madelung techniques[12], it can also be shown that the dipole interaction, restricted to the $\mathbf{q}=\mathbf{0}$ subspace, also takes the same form (for the *static* issues) but with H_0 slightly more important. We also elect to incorporate the interaction

$$H_3 = \frac{1}{8} \left(\sum_{\alpha} \hat{\mathbf{z}}_{\alpha} \cdot \hat{\mathbf{S}}_{\alpha} \right)^2 \quad (8)$$

which is generated by our projections. Treating these Hamiltonians as though they were initially functions of $\hat{\mathbf{J}}_{\alpha}$, applying the maximal spin projector then yields

$$H_4 \mapsto 16J^2 H_3 \quad H_0 \mapsto 4J^2 H_0 \quad H_3 \mapsto 4J^2 H_3 \quad (9)$$

All that remains for this case is H_0 and H_3 . Although the Hamiltonian H_0 is crucial for the original angular momentum, once we arrive at our spin-half pseudo-spin, this interaction reduces to a constant and can be ignored. As we only look at semi-classical solutions to our Hamiltonians, we are forced to keep H_0 active, although technically we need only the single Hamiltonian, H_3 , for this limit. Although H_0 is lost, there is still effectively a residual crystal-field interaction, H_3 , promoting the natural crystallographic directions, it is just no longer local. Spin-ice[7] is thought to be well represented by the maximal projected pseudo-spin. The spin component parallel to the crystallographic direction, $\hat{\mathbf{z}}_{\alpha} \cdot \hat{\mathbf{S}}_{\alpha}$, is then a conserved quantity and the pseudo-spin always points in these directions. The residual interaction energy on a tetrahedron is described by H_3 and is minimised by a ‘two-in and two-out’ configuration.

We will now consider the minimal spin-projector model. It is slightly more complicated to analyse but provides

$$H_4 \mapsto \left(J(J+1) + \frac{1}{4} \right) H_4 - 4 \left(J(J+1) - \frac{3}{4} \right) H_3 \\ H_0 \mapsto H_0 \quad H_3 \mapsto H_3 \quad (10)$$

The H_3 contribution now appears with the opposite sign. We observe that in the large J limit Eq.(10) becomes

$$H_4 - 4H_3 = \\ \frac{1}{12} \left[\left(\hat{S}_0^y - \hat{S}_1^y + \hat{S}_2^y - \hat{S}_3^y - \hat{S}_0^z + \hat{S}_1^z + \hat{S}_2^z - \hat{S}_3^z \right)^2 \right. \\ \left. + \left(\hat{S}_0^z - \hat{S}_1^z - \hat{S}_2^z + \hat{S}_3^z - \hat{S}_0^x - \hat{S}_1^x + \hat{S}_2^x + \hat{S}_3^x \right)^2 \right. \\ \left. + \left(\hat{S}_0^x + \hat{S}_1^x - \hat{S}_2^x - \hat{S}_3^x - \hat{S}_0^y + \hat{S}_1^y - \hat{S}_2^y + \hat{S}_3^y \right)^2 \right] \quad (11)$$

This provides a natural model which is minimised by

$$\hat{S}_0^x + \hat{S}_1^x - \hat{S}_2^x - \hat{S}_3^x = \hat{S}_0^y - \hat{S}_1^y + \hat{S}_2^y - \hat{S}_3^y \\ = \hat{S}_0^z - \hat{S}_1^z - \hat{S}_2^z + \hat{S}_3^z = A \quad (12)$$

There are many solutions to this, including the natural dipolar spirals (as found in $\text{Gd}_2\text{Sn}_2\text{O}_7$ [11]), the cubic symmetric triple- \mathbf{q} state and appropriate superpositions.

We now move on to exchange interactions. Susceptibility experiments suggest that there is a fairly strong antiferromagnetic interaction[23], and for a single tetrahedron this is

$$H_1 = \frac{1}{2} \left[\left(\hat{S}_0^x + \hat{S}_1^x + \hat{S}_2^x + \hat{S}_3^x \right)^2 \right. \\ \left. + \left(\hat{S}_0^y + \hat{S}_1^y + \hat{S}_2^y + \hat{S}_3^y \right)^2 \right. \\ \left. + \left(\hat{S}_0^z + \hat{S}_1^z + \hat{S}_2^z + \hat{S}_3^z \right)^2 \right] \\ \equiv \frac{1}{2} \hat{\mathbf{T}} \cdot \hat{\mathbf{T}} \quad (13)$$

defining a total-spin, $\hat{\mathbf{T}}$. Although we have chosen to use a pure isotropic interaction, the true interaction probably depends on the details of the occupied orbitals and is consequently likely to be more complicated. Employing our maximal spin projection this reduces to

$$H_1 \mapsto \frac{16}{3} J^2 (H_0 - H_3) \quad (14)$$

and, as expected, conflicts with ‘two-in and two-out’. In a similar way to the previous interaction we can consider

$$H_0 - H_3 = \frac{1}{24} \left[\left(\hat{S}_0^x + \hat{S}_0^y + \hat{S}_0^z - \hat{S}_1^x + \hat{S}_1^y + \hat{S}_1^z \right)^2 \right. \\ \left. + \left(-\hat{S}_2^x + \hat{S}_2^y - \hat{S}_2^z + \hat{S}_3^x + \hat{S}_3^y - \hat{S}_3^z \right)^2 \right. \\ \left. + \left(\hat{S}_0^x + \hat{S}_0^y + \hat{S}_0^z + \hat{S}_2^x - \hat{S}_2^y + \hat{S}_2^z \right)^2 \right. \\ \left. + \left(\hat{S}_1^x - \hat{S}_1^y - \hat{S}_1^z + \hat{S}_3^x + \hat{S}_3^y - \hat{S}_3^z \right)^2 \right. \\ \left. + \left(\hat{S}_0^x + \hat{S}_0^y + \hat{S}_0^z + \hat{S}_3^x + \hat{S}_3^y - \hat{S}_3^z \right)^2 \right. \\ \left. + \left(\hat{S}_1^x - \hat{S}_1^y - \hat{S}_1^z + \hat{S}_2^x - \hat{S}_2^y + \hat{S}_2^z \right)^2 \right] \\ = \frac{1}{16} \sum_{\alpha\beta} \left(\hat{\mathbf{z}}_{\alpha} \cdot \hat{\mathbf{S}}_{\alpha} - \hat{\mathbf{z}}_{\beta} \cdot \hat{\mathbf{S}}_{\beta} \right)^2 \quad (15)$$

which is the large-J limit. This is minimised by

$$\hat{S}_0^x + \hat{S}_0^y + \hat{S}_0^z = \hat{S}_1^x - \hat{S}_1^y - \hat{S}_1^z \\ = -\hat{S}_2^x + \hat{S}_2^y - \hat{S}_2^z = -\hat{S}_3^x - \hat{S}_3^y + \hat{S}_3^z = B \quad (16)$$

providing another natural Hamiltonian. Again there are many solutions to this, including all spins being both parallel and perpendicular to the natural crystallographic directions.

Applying the minimal spin projection to H_1 provides

$$H_1 \mapsto \left(J + \frac{1}{2}\right)^2 H_1 + \frac{4}{3} \left(J - \frac{1}{2}\right)^2 (H_0 - H_3) - \left(J^2 - \frac{1}{4}\right) H_2 \quad (17)$$

where

$$H_2 = \hat{\mathbf{T}} \cdot \sum_{\alpha} \hat{\mathbf{z}}_{\alpha} \left(\hat{\mathbf{z}}_{\alpha} \cdot \hat{\mathbf{S}}_{\alpha}\right) \quad (18)$$

Physically we see that the Heisenberg interaction remains dominant, but there are also terms equivalent to the maximal spin projector and additionally a new interaction, H_2 , that would vanish for an antiferromagnet. Note that the full dipolar interaction, restricted to a single tetrahedron, is proportional (up to a constant) to

$$H_4 + 6H_0 - 3H_2 + \frac{7}{3}H_1 \quad (19)$$

and so all these interactions are ‘expected’.

Our dipolar arguments naturally lead to H_0 , H_1 , H_2 , H_4 and (through pseudo-spin projection) H_3 , but our use of the Heisenberg interaction is less natural. There are likely to be uncontrolled orbitally driven distortions to the exchange process in this material. We are consequently forced into treating our Hamiltonian as phenomenological. Note that if for each exchange bond we simply enhance the bond when the spins are in the Cartesian plane of the bond, at the expense of when the spins are perpendicular to the plane, then we generate

$$\begin{aligned} H &= (1 - \delta) \left[\hat{S}_0^x \hat{S}_1^x + \hat{S}_2^x \hat{S}_3^x \right] \\ &+ (1 + \delta) \left[\hat{S}_0^y \hat{S}_1^y + \hat{S}_2^y \hat{S}_3^y + \hat{S}_0^z \hat{S}_1^z + \hat{S}_2^z \hat{S}_3^z \right] \\ &+ (1 - \delta) \left[\hat{S}_0^y \hat{S}_2^y + \hat{S}_1^y \hat{S}_3^y \right] \\ &+ (1 + \delta) \left[\hat{S}_0^z \hat{S}_2^z + \hat{S}_1^z \hat{S}_3^z + \hat{S}_0^x \hat{S}_2^x + \hat{S}_1^x \hat{S}_3^x \right] \\ &+ (1 - \delta) \left[\hat{S}_0^z \hat{S}_3^z + \hat{S}_1^z \hat{S}_2^z \right] \\ &+ (1 + \delta) \left[\hat{S}_0^x \hat{S}_3^x + \hat{S}_1^x \hat{S}_2^x + \hat{S}_0^y \hat{S}_3^y + \hat{S}_1^y \hat{S}_2^y \right] \\ &= H_1 - \delta H_4 - 2(1 - \delta) S^2 \end{aligned} \quad (20)$$

as desired in the next section. The spin-orbit interaction can easily bias the exchange, which is mediated by orbital overlaps, in this way.

One experimental observation that is problematic for the state currently proposed in the literature is the severely reduced moment. If the spins ordered in the proposed directions, perpendicular to the natural crystallographic axes, then one would expect to observe essentially the full moment, whereas a modest ordered moment fits the neutron Bragg data. The previously proposed explanation for this small moment is quantum fluctuations, but our prediction has different physics. We suggest that

the spins align quite close to the natural crystallographic directions, where the pseudo-spin states have a modest observable moment, as suggested by Eq.(5), in agreement with the experiments.

IV. SPINWAVES

We elect to use the Hamiltonian

$$H = J \sum_t [H_1 - \delta H_4 - \eta H_0 + \xi(H_0 - H_3)] \quad (21)$$

where t labels the tetrahedra, J is the natural energy scale, δ , η and ξ are scale-free parameters. We choose to use *positive* values for these parameters (to stabilise the multiple- \mathbf{q} states) and consequently one should probably view this Hamiltonian as phenomenological. The residual crystal-field interaction can account for η and ξ , but the choice of δ is physically opposite from the presumed dipolar source for this interaction.

This unexpected ‘failure’ of the dipolar interaction has direct experimental consequences. In real-space, point-size moments on a lattice have a dipolar energy proportional to

$$\mathcal{E}_D = -\frac{1}{2} \sum_{ii'} \hat{\mathbf{S}}_i \cdot \frac{\partial}{\partial \mathbf{x}} \hat{\mathbf{S}}_{i'} \cdot \frac{\partial}{\partial \mathbf{x}} V(|\mathbf{x}|) |_{\mathbf{x}=\mathbf{R}_i - \mathbf{R}_{i'}} \quad (22)$$

where $V(X)$ is the Coulomb potential between all lattice sites but vanishes as $X \mapsto 0$. In reciprocal space this transforms to

$$\mathcal{E}_D = \frac{1}{2} \sum_{\mathbf{k}} \sum_{\mathbf{G}} |(\mathbf{k} + \mathbf{G}) \cdot \hat{\mathbf{S}}_{\mathbf{k}}|^2 \tilde{V}(|\mathbf{k} + \mathbf{G}|) \quad (23)$$

where $\tilde{V}(K)$ is the Fourier transform of $V(X)$. Now since $V(X)$ is best represented as the Coulomb interaction multiplied by an increasing function, $\tilde{V}(K)$ corresponds to the Coulomb interaction multiplied by a reducing function. To minimise the dipolar interaction we should minimise the contributions from the Bragg spots, \mathbf{G} , closest to the origin. This means that the spin-density for these spots should be perpendicular to their reciprocal-space position. Interestingly, because neutrons scatter with essentially an equivalent dipolar interaction, this means that these spots should be *maximal* losing nothing from the orientational factor in neutron scattering[24]. In $\text{Gd}_2\text{Sn}_2\text{O}_7$, and to a slightly lesser extent in $\text{Gd}_2\text{Ti}_2\text{O}_7$, these Bragg spots are indeed maximal[11], whereas in $\text{Er}_2\text{Ti}_2\text{O}_7$ they are either small or almost vanishing. This tells us that the dipolar energy is intrinsically frustrated and explains why we are forced into using the apparently unphysical sign for H_4 .

Since the system exhibits long-range order, we elect to solve our Hamiltonian in the semi-classical limit to assess the expected style of order and associated magnons. We

employ the Holstein-Primakoff transformation[25]

$$\begin{bmatrix} \hat{S}^x \\ \hat{S}^y \\ \hat{S}^z \end{bmatrix} \mapsto \begin{bmatrix} \left[\frac{S}{2}\right]^{\frac{1}{2}} (b^\dagger + b) \\ \left[\frac{S}{2}\right]^{\frac{1}{2}} (b^\dagger - b) i \\ S - b^\dagger b \end{bmatrix} \quad (24)$$

with the z -axis oriented along the appropriate quantisation direction for each spin. We start out solving the case $\eta=0=\xi$ to find that the classical solution of Fig.1 denotes the ground-state manifold. This then provides

$$\hat{S}_0 = [\hat{x} \ \hat{y} \ \hat{z}] \begin{bmatrix} \cos \theta \cos \phi & -\sin \phi & \sin \theta \cos \phi \\ \cos \theta \sin \phi & \cos \phi & \sin \theta \sin \phi \\ -\sin \theta & 0 & \cos \theta \end{bmatrix} \begin{bmatrix} \hat{S}_0^x \\ \hat{S}_0^y \\ \hat{S}_0^z \end{bmatrix} \quad (25)$$

$$\hat{S}_1 = [\hat{x} \ \hat{y} \ \hat{z}] \begin{bmatrix} \cos \theta \cos \phi & -\sin \phi & \sin \theta \cos \phi \\ -\cos \theta \sin \phi & -\cos \phi & -\sin \theta \sin \phi \\ \sin \theta & 0 & -\cos \theta \end{bmatrix} \begin{bmatrix} \hat{S}_1^x \\ \hat{S}_1^y \\ \hat{S}_1^z \end{bmatrix} \quad (26)$$

$$\hat{S}_2 = [\hat{x} \ \hat{y} \ \hat{z}] \begin{bmatrix} -\cos \theta \cos \phi & \sin \phi & -\sin \theta \cos \phi \\ \cos \theta \sin \phi & \cos \phi & \sin \theta \sin \phi \\ \sin \theta & 0 & -\cos \theta \end{bmatrix} \begin{bmatrix} \hat{S}_2^x \\ \hat{S}_2^y \\ \hat{S}_2^z \end{bmatrix} \quad (27)$$

$$\hat{S}_3 = [\hat{x} \ \hat{y} \ \hat{z}] \begin{bmatrix} -\cos \theta \cos \phi & \sin \phi & -\sin \theta \cos \phi \\ -\cos \theta \sin \phi & -\cos \phi & -\sin \theta \sin \phi \\ -\sin \theta & 0 & \cos \theta \end{bmatrix} \begin{bmatrix} \hat{S}_3^x \\ \hat{S}_3^y \\ \hat{S}_3^z \end{bmatrix} \quad (28)$$

for any particular tetrahedron. Bloch transforming provides the excitations as

$$H = 2JS \sum_{\mathbf{k} \in K_+} [\mathbf{b}_\mathbf{k}^\dagger \ \mathbf{b}_{-\mathbf{k}}] \begin{bmatrix} A_\mathbf{k} & B_\mathbf{k} \\ B_\mathbf{k}^\dagger & A_\mathbf{k} \end{bmatrix} \begin{bmatrix} \mathbf{b}_\mathbf{k} \\ \mathbf{b}_{-\mathbf{k}}^\dagger \end{bmatrix} \quad (29)$$

where we are using the sublattice degrees of freedom as an implicit vector index and where K_+ denotes *half* of reciprocal-space, having divided out inversion. The matrices are explicitly

$$A_\mathbf{k} = \begin{bmatrix} 1 + 3\delta & -(\sin^2 \theta \cos^2 \phi + \delta)C_{y+z} & -(\sin^2 \theta \sin^2 \phi + \delta)C_{z+x} & -(\cos^2 \theta + \delta)C_{x+y} \\ -(\sin^2 \theta \cos^2 \phi + \delta)C_{y+z} & 1 + 3\delta & -(\cos^2 \theta + \delta)C_{x-y} & -(\sin^2 \theta \sin^2 \phi + \delta)C_{z-x} \\ -(\sin^2 \theta \sin^2 \phi + \delta)C_{z+x} & -(\cos^2 \theta + \delta)C_{x-y} & 1 + 3\delta & -(\sin^2 \theta \cos^2 \theta + \delta)C_{y-z} \\ -(\cos^2 \theta + \delta)C_{x+y} & -(\sin^2 \theta \sin^2 \phi + \delta)C_{z-x} & -(\sin^2 \theta \cos^2 \theta + \delta)C_{y-z} & 1 + 3\delta \end{bmatrix} \quad (30)$$

$$B_\mathbf{k} = \begin{bmatrix} 0 & (\cos \theta \cos \phi - i \sin \phi)^2 C_{y+z} & (\cos \theta \sin \phi + i \cos \phi)^2 C_{z+x} & \sin^2 \theta C_{x+y} \\ (\cos \theta \cos \phi - i \sin \phi)^2 C_{y+z} & 0 & \sin^2 \theta C_{x-y} & (\cos \theta \sin \phi + i \cos \phi)^2 C_{z-x} \\ (\cos \theta \sin \phi + i \cos \phi)^2 C_{z+x} & \sin^2 \theta C_{x-y} & 0 & (\cos \theta \cos \phi - i \sin \phi)^2 C_{y-z} \\ \sin^2 \theta C_{x+y} & (\cos \theta \sin \phi + i \cos \phi)^2 C_{z-x} & (\cos \theta \cos \phi - i \sin \phi)^2 C_{y-z} & 0 \end{bmatrix} \quad (31)$$

where

$$C_{\alpha \pm \beta} = \cos(k_\alpha \pm k_\beta) \quad (32)$$

We can now diagonalise this Hamiltonian with a Bogoliubov transformation to construct the spinwave spectrum, $E_{\mathbf{k}\alpha}$. In Fig.2 we look at the case where δ is very small. There are two almost flat bands on the energy scale of $2JS\sqrt{\delta}$. These control the original degeneracy of the Heisenberg model which has been lifted by the inclusion of H_4 . In Fig.3 we take the case of a small but relevant δ . We see that the flat bands have now developed a little dispersion and are close to the highest energy excitations. This plot has much in common with the experiments[2], but also has some clear problems. The low energy mode is clearly visible, as is the almost flat high energy mode, but instead of a linear dispersion at low energy we find a quadratic dispersion. This is because our model is actually degenerate across all the multiple- \mathbf{q} states of Fig.1, but if the particular ground-state were picked out by the energetics then the spinwave would be expected to

harden.

We are claiming that the low energy mode observed in the experiment is a rare form of longitudinal spinwave and so we now take time to explain this idea. We start out with an isotopic single- \mathbf{q} state, $\theta=0$, oriented along the z -axis. The magnetic scattering would then appear at (220), but the (022) and (202) spots would be absent. The usual Goldstone modes would be expected close to (002) and analogous spots on the body-centre-cubic superlattice generated by $\{(2\bar{2}\bar{2}), (\bar{2}2\bar{2}), (\bar{2}\bar{2}2)\}$, but there would usually be a spinwave gap at (200) and (020), as these points are non-magnetic and unrelated to (002) by any magnetic symmetry. The usual Goldstone modes are transverse; they are associated with the original state being tilted off axis and correspond to a small amount of magnetism at the same \mathbf{q} -point but in a perpendicular direction. The initially gapped modes at (200) and (020) correspond to small magnetic distortions of the other two styles of point-group related magnetism which are currently not present in the system. Physically they amount

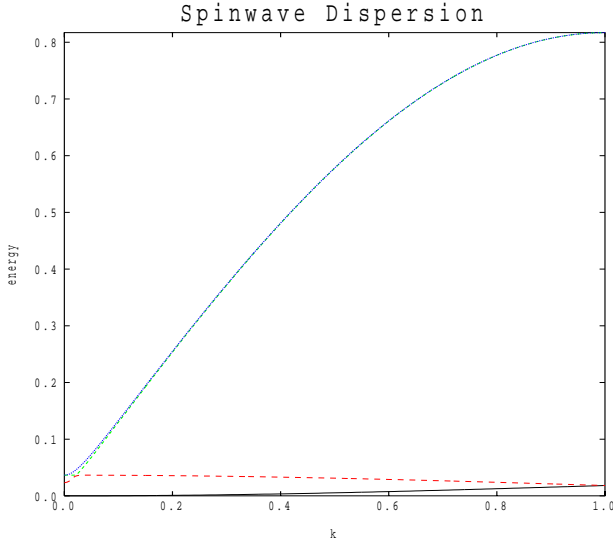


FIG. 2: The four spinwave branches for the case $\delta=0.0001$ in units of $2JS$, parallel to one of the Cartesian axes for the case corresponding to the experimentally proposed ground-state.

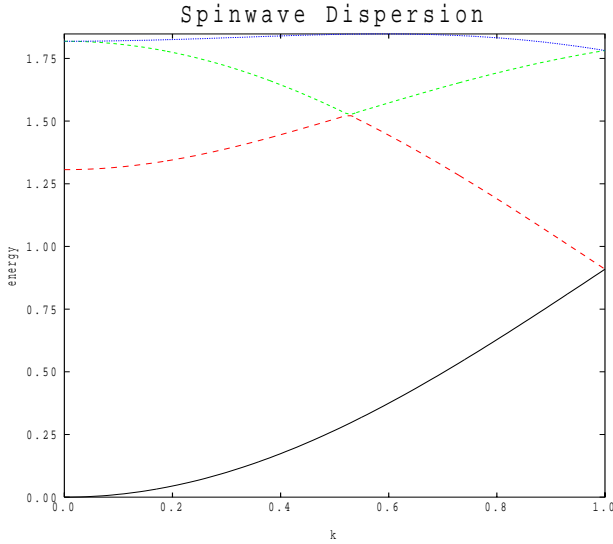


FIG. 3: The four spinwave branches for the case $\delta=0.2$ in units of $2JS$, parallel to one of the Cartesian axes for the case corresponding to the experimentally proposed ground-state.

to small changes in the ϕ and θ of Fig.1. The softening of these modes then corresponds to a *phase transition* from the original single- \mathbf{q} state into a multiple- \mathbf{q} state. The incoming state naturally uses ϕ to become a double- \mathbf{q} magnet or θ to become a triple- \mathbf{q} magnet[4]. In a normal rare-earth material the spin-orbit interaction opens a huge gap in the standard transverse mode, but the longitudinal mode, which links to the other magnetic states can be found at low energies, as in CeAs[18]. The phys-

ical idea is then that as the angle θ smoothly rotates, from zero at the single- \mathbf{q} state to $\cos \Theta = \frac{1}{\sqrt{3}}$ in the cubic triple- \mathbf{q} state, the mode remains at zero energy and

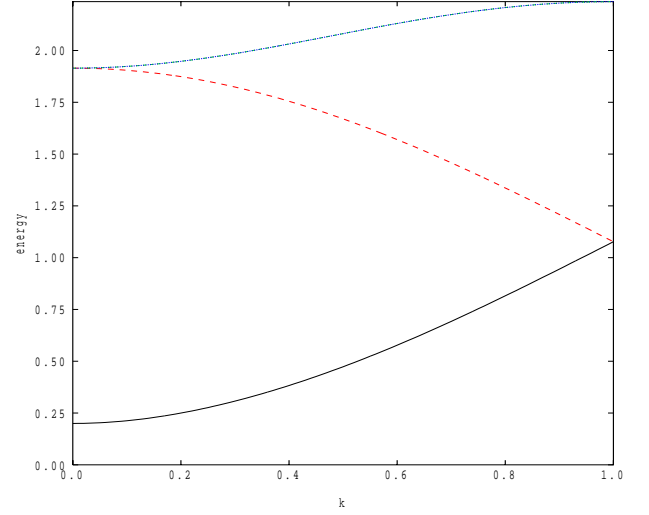


FIG. 4: The four spinwave branches for the case $\delta=0.2$, and $\eta=0.2$, which stabilises the cubic triple- \mathbf{q} state ($\phi = \frac{\pi}{4}$ and $\theta = \Theta$), in units of $2JS$, parallel to one of the Cartesian axes.

then generates a gap again in the cubic state. Including the parameter η into the spinwave calculation then stabilises the cubic triple- \mathbf{q} state and provides the gapped spin-wave dispersion of Fig.4.

We now take time to offer an exactly solvable model which highlights some of the issues

$$H = -\delta H_4 + \xi (H_0 - H_3) \quad (33)$$

This model also has the multiple- \mathbf{q} states of Fig.1 as its ground-state manifold, but it has the rather elementary dynamics controlled by

$$H = 2JS \begin{bmatrix} \left[\delta + \frac{\xi}{24} Z^* Z \right] C_{\mathbf{k}} & \frac{\xi}{24} Z Z C_{\mathbf{k}} \\ \frac{\xi}{24} Z^* Z^* C_{\mathbf{k}} & \left[\delta + \frac{\xi}{24} Z^* Z \right] C_{\mathbf{k}} \end{bmatrix} \quad (34)$$

where

$$C_{\mathbf{k}} = \begin{bmatrix} 3 & -C_{y+z} & -C_{z+x} & -C_{x+y} \\ -C_{y+z} & 3 & -C_{x-y} & -C_{z-x} \\ -C_{z+x} & -C_{x-y} & 3 & -C_{y-z} \\ -C_{x+y} & -C_{z-x} & -C_{y-z} & 3 \end{bmatrix} \quad (35)$$

and

$$Z = \cos \theta \sin \phi + i \cos \phi + \cos \theta \cos \phi - i \sin \phi - \sin \theta \quad (36)$$

The spinwave dispersion is given by

$$E_{\mathbf{k}\alpha} = 2JS \left[\delta \left(\delta + \frac{\xi}{12} \left[(\sin \theta \sin \phi - \cos \theta)^2 + (\cos \theta - \sin \theta \cos \phi)^2 + (\sin \theta \cos \phi - \sin \theta \sin \phi)^2 \right] \right) \right]^{\frac{1}{2}} \epsilon_{\mathbf{k}\alpha} \quad (37)$$

where

$$\epsilon_{\mathbf{k}\alpha} = 4, 4, 2 \pm [1 + 3\gamma_{\mathbf{k}}]^{\frac{1}{2}} \quad (38)$$

and $\gamma_{\mathbf{k}}$ is the face-centre-cubic structure factor for the underlying periodicity. The quantity $\epsilon_{\mathbf{k}\alpha}$ is essentially the pyrochlore lattice structure factor, exhibiting a gapless band and two flat bands describing the degeneracy (clear at finite energy). This model (ignoring the quadratic dependence at low energy) is enough to describe the observed inelastic neutron scattering[2], and hence this experiment does not clearly shed much light on *which* multiple- \mathbf{q} state might actually be stable.

Although all our multiple- \mathbf{q} states are classically degenerate, the quantum fluctuations lift this degeneracy[26] and tend to stabilise collinear states. For the current exactly solvable model we can calculate this quantum fluctuation energy analytically. At zero temperature we find that the fluctuation energy per spin, Q , is

$$Q = 3JS \left(-\delta - \frac{\xi}{24} |Z|^2 + \left[\delta \left(\delta + \frac{\xi}{12} |Z|^2 \right) \right]^{\frac{1}{2}} \right) \quad (39)$$

where

$$\begin{aligned} |Z|^2 &= 3 - (\sin \theta \cos \phi + \sin \theta \sin \phi + \cos \theta)^2 \\ &= (\sin \theta \sin \phi - \cos \theta)^2 + (\cos \theta - \sin \theta \cos \phi)^2 \\ &\quad + (\sin \theta \cos \phi - \sin \theta \sin \phi)^2 \end{aligned} \quad (40)$$

This fluctuation energy vanishes for the cubic triple- \mathbf{q} state and is minimised when the spins are perpendicular to the natural crystallographic directions. This exactly solvable model has very anisotropic interactions which do not promote standard collinear states. If we accept that our spin is pseudo-spin half and that the quantum fluctuation energy is of the same order as the classical energy, then we can now attempt a physical explanation for the system. If there is a classical energy promoting the cubic triple- \mathbf{q} state, such as H_0 or H_3 , then this could balance the quantum fluctuation energy at the observed experimental state. However, careful analysis of the current model shows that the state jumps discontinuously from the cubic state to one with the spins perpendicular to the crystallographic directions and so the current model is too simplistic.

Returning to our more physical model, $H_1 - \delta H_4$, we can calculate the quantum fluctuation energy as

$$Q = JS \left(-1 - 3\delta + \frac{1}{4N} \sum_{\mathbf{k}\alpha} E_{\mathbf{k}\alpha} \right) \quad (41)$$

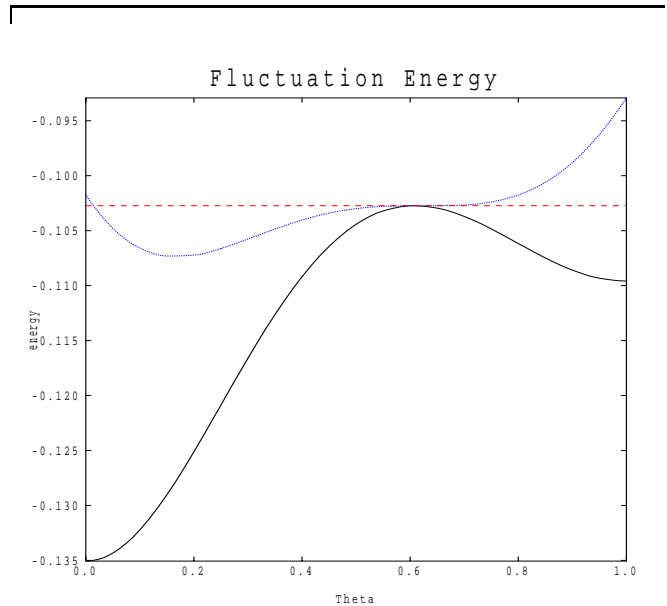


FIG. 5: The quantum fluctuation energy for the case $\delta=0.2$, as a function of θ (in units of $\frac{\pi}{2}$) with $\phi=\frac{\pi}{4}$ (solid curve). We have included a small η to achieve the blue curve.

at zero temperature, and we offer an example in Fig.5. As expected, the ground-state is now the single- \mathbf{q} state (black curve). We next add a carefully scaled classical contribution favouring the cubic state and now an intermediate state appears relatively stable (blue curve). However the energetics are not very ‘stable’ and rather than continuing to evolve smoothly, the ground-state tends to make a small discontinuous jump when close to the cubic state, to the cubic state.

Having analysed a particular case, we now move on to generalities. Our complete Hamiltonian is

$$H = J \sum_t \left[\alpha H_1 - \delta H_4 - \eta H_0 + \xi (H_0 - H_3) - \frac{3}{2} \beta H_2 + \epsilon H_5 \right] \quad (42)$$

where H_5 is a local interaction which lifts the azimuthal symmetry and provides a crystal-field preference appropriate to the weak hexagonal symmetry around the natural crystallographic directions. We can semi-classically solve such an interaction in general. There are four natural ground-states: the dipolar spirals[11], a generalised ‘two-in and two-out’ state (typical for spin-ice[7]), the pure triple- \mathbf{q} state[4] and finally a multiple- \mathbf{q} state with the spins perpendicular to the natural crystallographic directions, but pointing along one of the twelve natural directions allowed by the weak hexagonal interaction. The key observation is that in *all* of these phases there

is a natural gap in the spinwave spectrum. Our generic Hamiltonian is very anisotropic and that generates the expected loss of continuous symmetry and a consequent gap. The observed gapless state is truly unexpected.

There is no easy way to eliminate the gap in the spiral and ‘two-in and two-out’ phases, but since $\text{Er}_2\text{Ti}_2\text{O}_7$ has a multiple- \mathbf{q} ground-state this is irrelevant. One way to close the gap is to omit the hexagonal crystal-field interaction, $\epsilon \mapsto 0$. This is the current core of the picture prevalent in the literature[1–3, 15]. If it were exact, then one could use a magnetic field to access this degeneracy but the current experiments point to the particular azimuthal angle being pinned and nonreactive to a field. A weak hexagonal field provides a small gap. However it is possible that the observed linear dispersion, and specific heat, have not been accessed at low enough energies, and temperatures respectively, to observe this gap. Another way to close the gap, our explanation, is that the multiple- \mathbf{q} degeneracy is active. We would leave the hexagonal interaction, which stabilises $\phi = \frac{\pi}{4}$, but omit the excess local crystal-field term, $\eta \mapsto 0$. The inclusion of the hexagonal interaction removes one inconsistency in our model; the quadratic dispersion at low energy becomes linear as required, and our continuous degeneracy is in the angle θ and not ϕ . We believe that once the particular choice of θ is chosen by some collective compromise, the gaplessness still remains. Since there is no such collective competition in our semi-classical analysis, we have resorted to suggesting that quantum fluctuations could provide such an asymmetric θ , without offering any rigorous calculations to prove this.

V. CONCLUSIONS

Rare-earth magnets are usually very anisotropic with a gap to magnetic excitations. $\text{Er}_2\text{Ti}_2\text{O}_7$ is an unusual example of a gapless rare-earth magnet. The experimental evidence points towards a multiple- \mathbf{q} antiferromagnet where the spins do not point along crystallographically natural directions. The low energy mode then smoothly varies this incommensurate angle. The single-domain single-crystal measurements indicate that the angles $\phi = \frac{\pi}{4}$ and (the incommensurate) $\theta \sim \frac{\pi}{5}$ are selected.

The observed spinwave spectrum is well represented by the natural pyrochlore structure factor and hence does not restrict the model much, except that the spectrum is gapless and so a continuous degeneracy is required. The observed orientational factors in the neutron scattering are contradictory to the expectations of the dipolar interaction and this leads us to propose the model with the opposite sign for H_4 in order to fit the experiments.

Our physical insight arises from the balance between quantum fluctuations and classical interactions. Our Hamiltonian, $H_1 - \delta H_4$, is classically degenerate, with the states of Fig.1 as the ground-state manifold. The quan-

tum fluctuations stabilise the single- \mathbf{q} state, and because the pyrochlore lattice is highly frustrated the quantum fluctuation energy is expected to be large. Due to the strong spin-orbit and crystal-field effects there are additional interactions which happen to favour the natural crystallographic directions. If we imagine increasing such an interaction smoothly from zero, at some strength it will overturn the quantum fluctuation energy and drive the system into a multiple- \mathbf{q} state. We are proposing that this transition would be second-order and would pass through the intermediate gapless phases where θ varies from zero to Θ , with $\text{Er}_2\text{Ti}_2\text{O}_7$ part-way through this process at the observed value of $\theta \sim \frac{\pi}{5}$.

Our proposal requires a multiple- \mathbf{q} state with an unnatural angle θ which is not clearly derived nor convincingly explained. The current picture in the literature has the natural angles $\theta = \frac{\pi}{2}$ and $\phi = \frac{\pi}{4}$ and so would be expected to have a gap. This gap needs to be too small to be observed. This state should also have a dominant (111) spot, as this Bragg spot structure factor is perpendicular to its momentum transfer, whereas the spot is observed to be small. The only weakness in our argument is the form-factor, which would have to have a severe and unexpected orientational dependence.

There are now two plausible states that will fit the experiments: the original idea[15], with spins perpendicular to the natural crystallographic directions, and our proposal with a non-symmetric angle θ . How can we decide between them experimentally? The original proposal should exhibit a gap, controlled by the hexagonal crystal field, which can be sought. If this gap is tiny, then an external magnetic field should be able to rotate the angle ϕ and dramatically change the magnetic Bragg scattering, with the ratio of intensities changing from (1, 1, 4) to (3, 3, 0) for the three main Bragg spots. One would also need an explanation for why the (111)-type Bragg spots were so small, either from dramatic form-factor dependence or from some other as yet unresolved experimental issue. Our proposal has rather different issues. Since we fit the known data the experiments are not too pertinent, it is the theory that is critical. We need a model that stabilises the unsymmetric state and we need the state to remain gapless, both issues having been side-stepped in this article.

Our proposed model is a pseudo-spin half model on the pyrochlore lattice but our semi-classical magnetic techniques are not sophisticated enough to predict our expectations. Better theoretical analysis of the quantum mechanical model is required to make a more detailed comparison with experiment.

Acknowledgments

We wish to acknowledge useful discussions with E.A. Blackburn.

-
- [1] J.D.M. Champion, M.J. Harris, P.C.W. Holdsworth, A.S. Wills, G. Balakrishnan, S.T. Bramwell, E. Cizmar, T. Fennell, J.S. Gardner, J. Lago, D.F. McMorro, M. Orendac, A. Orendacova, D. McK. Paul, R.I. Smith, M.T.F. Telling and A. Wildes, *Phys. Rev.* **B68** 020401(R) (2003);
- [2] J.P.C. Ruff, J.P. Clancy, A. Bourque, M.A. White, M. Ramazanoglu, J.S. Gardner, Y. Qiu, J.R.D. Copley, M.B. Johnson, H.A. Dabkowska and B.D. Gaulin, *Phys. Rev. Lett.* **101** 147205 (2008);
- [3] H.B. Cao, I. Mirebeau, A. Gukasov, P. Bonville and C. Decorse, *Phys. Rev.* **B82** 104431 (2010);
- [4] M.W. Long, *Int. J. of Mod. Phys.* **B7** 2981 (1993);
- [5] S. Rosenkranz, A.P. Ramirez, A. Hayashi, R.J. Cava, R. Siddharthan and B.S. Shastry, *J. Appl. Phys.* **87** 5914 (2000); Unpublished;
- [6] H.W.J. Blote, R.F. Wielinga and W.J. Huiskamp, *Physica* **43** 549 (1969);
- [7] S.T. Bramwell and M.J.P. Gingras, *Science* **294** 1495 (2001);
- [8] C. Castelnovo, R. Moessner and S.L. Sondhi, *Nature (London)* **451** 42 (2008);
- [9] J. Villain, *Z. Phys.* **B33** 31 (1979);
- [10] J.D.M. Champion, A.S. Wills, T. Fennell, S.T. Bramwell, J.S. Gardner and M.A. Green, *Phys. Rev.* **B64** 140407(R) (2001); J.R. Stewart, G. Ehlers, A.S. Wills, S.T. Bramwell and J.S. Gardner, *J. Phys.: Condens. Matter* **16** L321 (2004);
- [11] A.S. Wills, M.E. Zhitomirsky, B. Canals, J.P. Sanchez, P. Bonville, P. Dalmas de Réotier and A. Yaouanc, *J. Phys.: Condens. Matter* **18** L37 (2006);
- [12] N.P. Radu, M. Dion, M.J.P. Gingras, T.E. Mason and J.E. Greedan, *Phys. Rev.* **B59** 14489 (1999);
- [13] V.N. Glazkov, M.E. Zhitomirsky, A.I. Smirnov, H.-A. Krug von Nidda, A. Loidl, C. Marin and J.-P. Sanchez, *Phys. Rev.* **B72** 020409(R) (2005);
- [14] R. Siddharthan, B.S. Shastry, A.P. Ramirez, A. Hayashi, R.J. Cava and S. Rosenkranz, *Phys. Rev. Lett.* **83** 1854 (1999);
- [15] J.D.M. Champion and P.C.W. Holdsworth, *J. Phys.: Condens. Matter* **16** S665 (2004);
- [16] S.S. Sosin, L.A. Prozorova, M.R. Lees, G. Balakrishnan and O.A. Petrenko, *Phys. Rev.* **B82** 094428 (2010);
- [17] A. Gozar, B.S. Dennis, G. Blumberg, S. Komiya and Y. Ando, *Phys. Rev. Lett.* **93** 027001 (2004);
- [18] B. Halg and A. Furrer, *Phys. Rev.* **B34** 6258 (1986);
- [19] A. Poole, A.S. Wills and E. Lelievre-Berna, *J. Phys.:Condens. Matter* **19** 452201 (2007); H. Cao, A. Gukasov, I. Mirebeau, P. Bonville, C. Decorse and G. Dhahlenne, *Phys. Rev. Lett.* **103** 056402 (2009);
- [20] G.H. Lander and M.S.S. Brooks, *Phys. Rev.* **B43** 13672 (1991);
- [21] G.H. Lander and W.G. Stirling, *Phys. Rev.* **B21** 436 (1980);
- [22] P. Giannozzi and P. Erdos, *J. Magn. Magn. Mat.* **67** 75 (1987);
- [23] P. Dasgupta, Y. Jana and D. Ghosh, *Solid State Commun.* **139** 424 (2006);
- [24] S.W. Lovesey, "Theory of Neutron Scattering from Condensed Matter", (Oxford University Press, Oxford, 1984);
- [25] T. Holstein and H. Primakoff; *Phys. Rev.* **58** 1098 (1940);
- [26] M.W. Long, *J. Phys.:Condens. Matter* **1** 2857 (1989);